

A flow-system array for the discovery and scale up of inorganic clusters

Craig J. Richmond¹, Haralampos N. Miras¹, Andreu Ruiz de la Oliva¹, Hongying Zang¹, Victor Sans¹, Leonid Paramonov², Charalampos Makatsoris², Ross Inglis³, Euan K. Brechin³, De-Liang Long¹ and Leroy Cronin^{1*}

The batch synthesis of inorganic clusters can be both time consuming and limited by a lack of reproducibility. Flow-system approaches, now common in organic synthesis, have not been utilized widely for the synthesis of clusters. Herein we combine an automated flow process with multiple batch crystallizations for the screening and scale up of syntheses of polyoxometalates and manganese-based single-molecule magnets. Scale up of the synthesis of these architectures was achieved by programming a multiple-pump reactor system to vary reaction conditions sequentially, and thus explore a larger parameter space in a shorter time than conventionally possible. Also, the potential for using the array as a discovery tool is demonstrated. Successful conditions for product isolation were identified easily from the array of reactions, and a direct route to 'scale up' was then immediately available simply by continuous application of these flow conditions. In all cases, large quantities of phase-pure material were obtained and the time taken for the discovery, repetition and scale up decreased.

The benefits of continuous-flow processing in synthetic organic chemistry have been well researched and documented in recent years^{1,2}. Key advantages include higher efficiencies of heat transfer and rapid homogeneous mixing, which lead to increased reaction rates, yields and selectivities^{3,4}. Also, techniques for continuous-flow processes have proved useful in inorganic synthesis, but examples are limited mainly to the production of metallic and semiconductor nanoparticles and quantum dots⁵. Other major areas of interest in inorganic chemistry, such as polyoxometalates (POMs)^{6,7} and coordination clusters (especially those with interesting magnetic properties, such as single-molecule magnets (SMMs))^{8–12}, typically utilize batch syntheses and purification via crystallization. Screening of reaction conditions for the reproduction and scale up of novel architectures must therefore cover a large area of synthetic space as it not only has to achieve conditions suitable for the target formation, but also those for target crystallization. Large-number reaction arrays are therefore an inherent aspect in this process, which can be an extremely laborious and time-consuming task when working solely under batch conditions, especially in exploring delicate multiparameter self-assembly reactions aimed to produce supramolecular architectures. Indeed, the size of the parameter space can be so vast that even after a chance 'batch discovery', the re-discovery and scale up of the process to produce more than a few crystals of the product can be almost impossible on a limited timescale. As such, this presents a critical bottleneck to the reliable synthesis of inorganic macromolecules with scientifically and technologically important physical properties, and this lack of phase-pure material prevents a rigorous investigation of the physical properties or exploitation of the properties in real-world devices and applications.

Herein the combination of autonomous flow processing with multiple batch crystallizations is presented as a new and efficient method to create large-number reaction arrays for rapidly scanning large areas of reaction-parameter space to increase the probability of

discovering new materials. Additionally, this flow-based approach for the generation of multiple batch reactions was exploited for the continuous production of identical batch reactions required to scale up the isolated materials. As an initial proof of concept, a set-up with a multiple-pump reactor was applied in the production of a selection of polyoxomolybdates of various sizes and structural complexity, {Mo_x} compounds **1** to **6** (Fig. 1)^{13–16}. To further demonstrate the scope of the method, the syntheses of a number of coordination clusters with SMM properties were also explored, {Mn_x} compounds **7** to **10** (see Fig. 5)^{17–20}.

After screening the reaction parameters for each target compound **1–6**, the optimal conditions for product crystallization showed good agreement with those of the original batch procedures, although compound **6** is reported here for the first time. The set-up utilized 12 programmable syringe pumps (see Methods), although this is extendable to 15 in our system, and a LabVIEWTM-based PC interface was used to control the pumps (Fig. 1).

The reagent set chosen for POM synthesis consisted of distilled deionized water for dilution, 2.5 M Na₂MoO₄ as the molybdenum source, three acid sources (5.0 M HCl, 1.0 M H₂SO₄ and 50% AcOH), 4.0 M NH₄OAc and two sources of reducing agent, 0.25 M Na₂S₂O₄ and saturated (0.23 M) N₂H₄·H₂SO₄. For the simplest POM target, compound **1** {Mo₃₆}, only three of the 12 pumps were required to vary incrementally the relative flow rates of the water, molybdate and HCl stock solutions; for compounds **2** {Mo₁₅₄}, **3** {Mo₁₃₂}, **4** {Mo₁₀₂} and **5** {Mo₃₆₈} up to five pumps were required to supply the additional reducing-agent and buffer stocks.

The first-reported synthesis of the {Mo₃₆} structure by Krebs simply involved acidifying an aqueous solution of sodium molybdate, which subsequently precipitated crystals of the target compound¹³. However, as with most syntheses, only the best synthetic conditions are reported and the arduous work that went into finding them is glossed over, if even mentioned at all. Therefore

¹WestCHEM, School of Chemistry, University of Glasgow, University Avenue, Glasgow G12 8QQ, UK, ²School of Engineering and Design, Brunel University, Uxbridge, Middlesex UB8 3PH, UK, ³School of Chemistry, University of Edinburgh, Kings Buildings, Edinburgh EH9 3JJ, UK. *e-mail: Lee.Cronin@glasgow.ac.uk

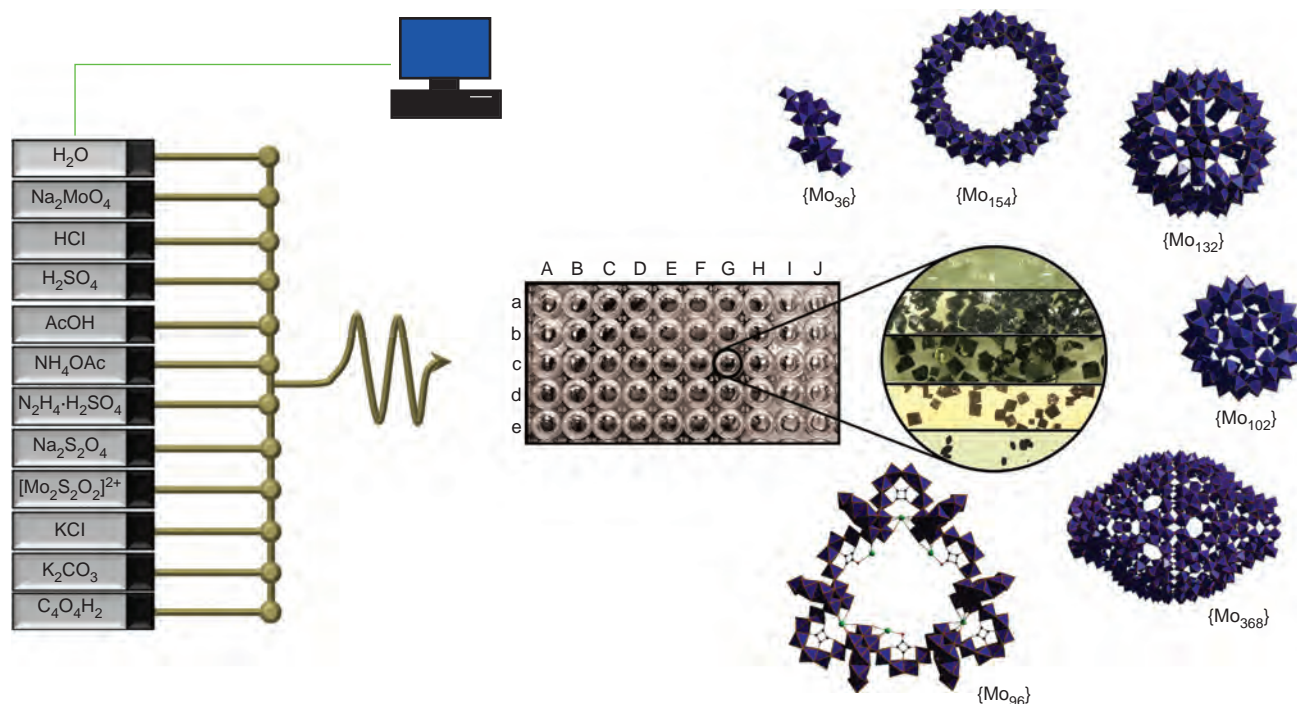


Figure 1 | Reaction input parameters were altered to generate reaction arrays to be screened for the crystallization of polyoxomolybdate targets.

A schematic of the pump set-up and reagent inputs (left) leads to a representative image of the 5×10 reaction-array outputs (centre). $C_2O_4H_2$, squaric acid. During the screening process for each target, crystal batches were obtained in a handful of reactions in which the flow conditions produced the reaction conditions required for successful crystallization. Images of crystal batches and polyhedral structural representations for the target polyoxomolybdates are shown (right). The truncated molecular formulae in parentheses represent the following complete formulae: $\{Mo_{36}\}$ (1) = $Na_8[Mo_{36}O_{112}(H_2O)_{16}] \cdot 58H_2O$, $\{Mo_{154}\}$ (2) = $Na_{15}[Mo(v)_{126}Mo(v)_{28}O_{462}H_{14}(H_2O)_{70}]_{0.5}[Mo(v)_{124}Mo(v)_{28}O_{457}H_{14}(H_2O)_{68}]_{0.5} \cdot \sim 400H_2O$, $\{Mo_{132}\}$ (3) = $(NH_4)_{42}[Mo(v)_{72}Mo(v)_{60}O_{372}(CH_3COO)_{30}(H_2O)_{72}] \cdot \sim 300H_2O \cdot \sim 10CH_3COONH_4$, $\{Mo_{102}\}$ (4) = $Na_{12}[Mo(v)_{72}Mo(v)_{30}O_{282}(SO_4)_{12}(H_2O)_{78}] \cdot \sim 280H_2O$, $\{Mo_{368}\}$ (5) = $Na_{48}[H_xMo_{368}O_{1032}(H_2O)_{240}(SO_4)_{48}] \cdot \sim 1,000H_2O$ and $\{Mo_{96}\}$ (6) = $(N(CH_3)_4)_6K_{30}[(Mo_2O_2S_2)_3(OH)_4(C_4O_4)]_9[(Mo_2O_2S_2)_2(OH)_2(C_4O_4)]_3(Mo_5O_{18})_6 \cdot 600H_2O$.

our focus was to prepare a simple pump set-up that could repeat this screening process but with minimal human input. With $\{Mo_{36}\}$ in mind as a primary target for our 'screening array', the pumps were programmed to run at a range of flow rates, incrementally increasing both the relative ratio of acid to molybdate and the overall reagent concentrations (two key parameters of POM formation and crystallization) throughout the experimental run.

As shown in Fig. 2, the volume of acid with respect to Mo was varied from 0% to 90% (across rows) and the volume of additional water with respect to the total reagent volume was varied from 80% to 0% (down columns). Independent variation of just these two parameters resulted in the creation of 50 distinct reaction batches with the potential to crystallize the $\{Mo_{36}\}$ target. The combined flow rate for all pumps running at any specific point was set to 12.5 ml min^{-1} to maintain a consistent output flow velocity and reaction volume, and the variation of the output-flow composition was controlled by varying the rates of the individual pumps relative to one another. The manifold employed was of nine-port 1/8 inch (3.175 mm) design made of polyether ether ketone (PEEK). A length of tubing (6.22 m) of relatively wide bore (1.6 mm internal diameter) was placed after the mixing manifold to allow dissolution before the collection of transient precipitates typically observed on acidification of molybdate salts. The diameter was chosen to be sufficiently wide to avoid blockage of the system with the formation of such precipitates and the tubing length was chosen to coincide with the reaction volumes collected. The tube was made of fluorinated ethylene propylene (FEP) and employed as a chemical reactor without further modification. After each reaction array the tube was cleaned with an aqueous solution of NaOH and distilled water. A pulse-tracer experiment used to assess the flow patterns

within the reactor showed a combination of plug flow with some degree of back mixing, which is consistent with the parabolic profile established under laminar conditions²¹. The relative flow rates were changed every 30 seconds, and thus gave a reaction volume of 6.25 ml (that is, 0.5 minutes \times 12.5 ml min^{-1}) for each reaction composition and the total volume for the tubing was 12.5 ml (that is, two reaction volumes or one minute of residence time). The individual reaction mixtures were collected every 30 seconds with a 1.5 second delay to allow the test tubes to be changed during collection. An entire run of 50 reactions, which scanned conditions from high to low dilution and from high to low pH, therefore took less than 35 minutes to complete.

As confirmation that the reaction mixture compositions matched the theoretical values from the programmed flow rates, the pH of the individual reactions within the 'reaction array' was measured immediately after collection (Fig. 3a). The pH fluctuated from high to low periodically across the array of reactions, which maps directly to the conditions imposed by the pre-programmed screening sequence (Fig. 2): reaction number 1 (or aA from Fig. 2) contained no acid and the dilution factor was 8:2. Hence 80% of the reaction volume came purely from the water stock and the remaining 20% from the 2.5 M Na_2MoO_4 stock, and the relatively high measured pH of about 6–7 is consistent with a solution of this composition. From reactions 2 to 10 (or aB to aJ) the overall trend was a gradual decrease in pH as the acid content increased with respect to the Mo, with the dilution factor remaining constant at 8:2. For reaction number 11 (bA) the pH jumped back up as the flow rates reverted back to 0% acid, but now at a slightly higher Mo concentration because of the decreased dilution factor of 6:4. This trend was repeated across the remainder of the array as the

	Flow rate ratios		Acid:Molybdenum ratio									
	H ₂ O	Reagents	0:10	1:9	2:8	3:7	4:6	5:5	6:4	7:3	8:2	9:1
			A	B	C	D	E	F	G	H	I	J
a	8	2										
b	6	4										
c	4	6										
d	2	8										
e	0	10										

Figure 2 | Arbitrary ratios of reagent flow rates used to create the 5 × 10 reaction arrays for screening of the syntheses of {Mo₃₆} (1) and {Mo₁₅₄} (2). As one moves down rows a–e the dilution factor decreases, as dictated by the decreasing ratio of flow rates for the water pump versus all other reagents; this is indicated by the dimpled shading, where the lighter colours indicate lower concentrations and stronger colours higher concentrations. Across columns A–J the ratios of the pump rates for the acid versus molybdate increase and the reactions become more acidic, indicated by the colour gradient based on the universal pH indicator scale (that is, red is acidic and blue is basic). One programmed reaction run automatically scans 50 reactions that range from high to low pH (blue to red) and low to high reagent concentration (light to strong).

acid:Mo ratio and dilution factor varied as dictated by the pre-programmed screening sequence.

After leaving the solutions undisturbed and open to air for 24 hours, three out of the 50 reactions had precipitated colourless columnar crystals: reaction numbers 26 (cF), 36 (dF) and 46 (eF). Single-crystal X-ray diffraction and infrared spectroscopy were used to confirm the crystalline product as pure {Mo₃₆}. The conditions under which the crystalline product was synthesized were of low pH and high Mo concentration, consistent with those of the traditional batch synthesis¹³. The remaining 47 reaction solutions remained either as colourless solutions or precipitated an amorphous white powder. For those reactions that remained colourless solutions, an attempt was made to identify the condensed molybdate species in the solution from dynamic light scattering measurements taken of the reaction solutions (see Supplementary Fig. S3). Particle sizes of 1.7–2 nm were observed consistently for the more-dilute solutions at low pH, which indicates the formation of a condensed molybdenum species of similar size to {Mo₃₆}. Indeed, after leaving some of these solutions for a few more days, a handful of colourless columnar crystals formed, which were also confirmed as {Mo₃₆} by crystallographic unit-cell matching.

The next target structure for the screening array was the reduced ‘molybdenum blue wheel’ 2 {Mo₁₅₄}, first characterized by Müller *et al.*^{22,23}, and produced in batch via the partial reduction of an acidified molybdate solution with a reducing agent such as sodium dithionite. An additional pump that contained a solution of 0.25 M Na₂S₂O₄ was therefore programmed to provide a 10 mol% reducing agent with respect to Mo during the scanning of the reaction parameters, where again the relative reagent ratios and levels of dilution were altered incrementally throughout the experimental run. The flow rate of the dithionite pump was set to scale directly with that of the molybdate pump, which thus gave a constant reduction environment for all 50 reactions. The flow rate for the reducing-agent pump could have been set as a new variable parameter, but it is well known that increasing this value beyond 10 mol% results in increased levels of amorphous polymeric molybdenum oxide species¹⁴ and so would have increased the array dimensions without increasing the potential to isolate high-quality crystalline products suitable for X-ray structure determination. A similar pattern in the pH values measured for the {Mo₁₅₄} reaction discovery array was observed; as expected, the pH fluctuated across the array as the acid content and dilution ratios varied in accordance with the pre-programmed rates of reagent flow (Fig. 3b).

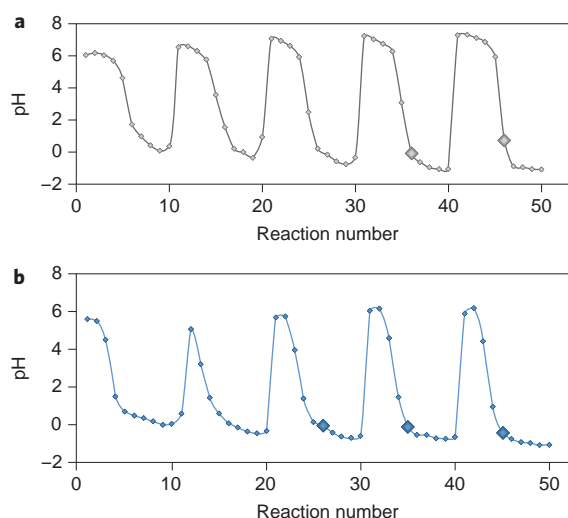


Figure 3 | Charts of pH measurements for the 5 × 10 screening arrays. a,b {Mo₃₆} synthesis (a) and {Mo₁₅₄} synthesis (b). The pH varies periodically in all cases as the ratios of the flow rates for the acids/molybdate increase for each dilution factor. The reaction number corresponds to fractions being collected sequentially as five rows of ten in the 50-reaction array created from the corresponding flow rates in Fig. 2 (that is, 1–10 is aA–aJ, 11–20 is bA–bJ, 21–30 is cA–cJ, 31–40 is dA–dJ and 41–50 is eA–eJ). Data points for reactions that result in successful crystallization are highlighted.

The 50 reactions from the array were again left undisturbed for 24 hours before they were checked for successful crystallization. Again, three out of the 50 reactions precipitated crystalline material, reaction numbers 26 (cF), 35 (dE) and 45 (eE), and the remaining reactions precipitated either no material or a dark amorphous material not suitable for crystallographic analysis. As before, the low pH and high Mo concentrations that gave a successful product isolation were consistent with the original batch conditions and the crystalline products were confirmed as {Mo₁₅₄} by crystallographic unit-cell checks and by infrared and absorbance spectroscopy¹⁴. In addition to the pH measurements, absorbance

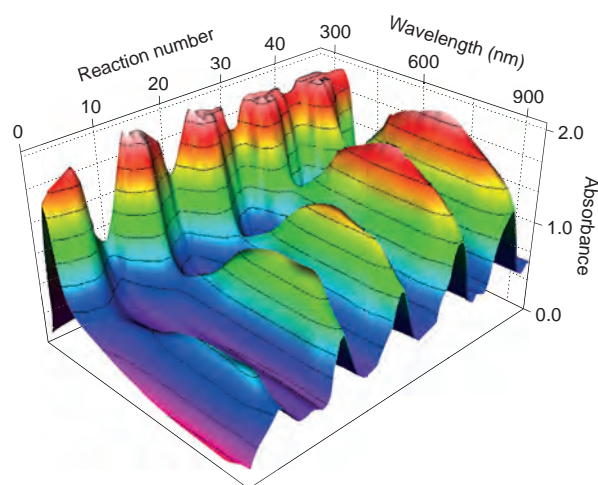


Figure 4 | Plot of ultraviolet-visible absorbance for diluted fractions of an {Mo₁₅₄} reaction array that shows a similar periodic trend to the pH. The reaction number corresponds to fractions being collected sequentially as five rows of ten in the 50-reaction array created from the corresponding flow rates in Fig. 2 (that is, 1–10 is aA–aJ, 11–20 is bA–bJ, 21–30 is cA–cJ, 31–40 is dA–dJ and 41–50 is eA–eJ). Samples were diluted in a ratio of 1:16 with distilled water and filtered before absorbance measurements were taken.

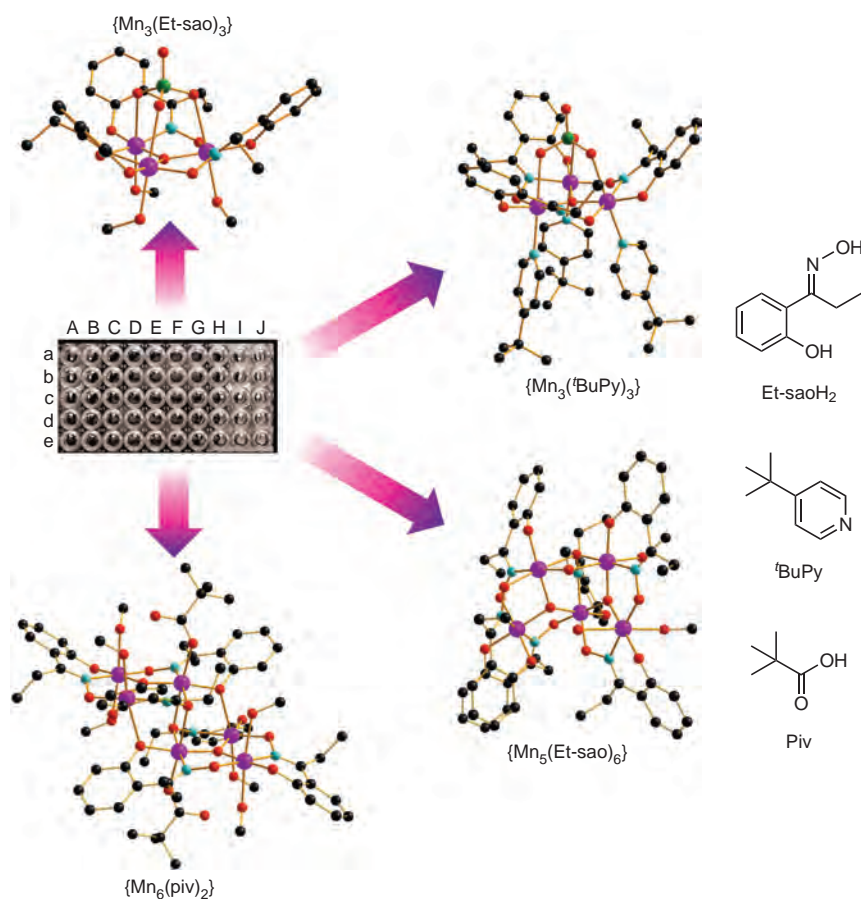


Figure 5 | The reagent inputs to the flow-system array were switched to those relevant for the syntheses of manganese-based SMMs. A family of polynuclear manganese complexes were synthesized successfully. $\{Mn_3(Et-sao)_3\}$ (**7**) = $Mn_3O(Et-sao)_3(MeOH)_3(ClO_4)$, $\{Mn_3(tBuPy)_3\}$ (**8**) = $Mn_3O(Et-sao)_3(tBuPy)_3(ClO_4)$; $\{Mn_5(Et-sao)_6\}$ (**9**) = $Mn_5O_2(Et-sao)_6(MeO)(H_2O)(MeOH)_2$ and $\{Mn_6(piv)_2\}$ (**10**) = $Mn_6O_2(Et-sao)_6(piv)_2(MeOH)_6$. Structures of the manganese complexes obtained are shown in their ball-and-stick representation (Mn = magenta, Cl = green, N = light blue, O = red, C = black); hydrogen atoms are omitted for clarity. The structures of the ligands used as reagent inputs are also given on the right.

spectroscopy was used to monitor the change in the reaction composition across the reaction array. Figure 4 shows a 3D plot of the absorbance spectra for the 5×10 reaction array. The absorbance at ~ 750 nm (indicative of Mo-blue species)¹⁴ was observed to coincide with the periodic fluctuations in pH, which again demonstrates that the resulting reaction conditions were consistent with the pre-programmed flow rates.

Next, compound **3**, the spherical $\{Mo_{132}\}$ Keplerate cluster¹⁵, was targeted, which required the operation of the AcOH and NH_4OAc reagent pumps in place of the HCl pump and the use of $N_2H_4 \cdot H_2SO_4$ in place of $Na_2S_2O_4$. The ratio of NH_4OAc to AcOH flow rates was set to 1:1 to provide a buffered solution of about pH 4. The array experiment was then run as before, with the ratio of reduced molybdenum/buffer reagents altered in addition to the level of dilution. The amount of reducing agent was set at 20 mol% in accordance with the approximate ratio of Mo(v):Mo(vi) in the $\{Mo_{132}\}$ target. The pH of the reactions within the array again varied periodically, but over the narrower pH range of about 4–5 because acetate buffer stocks were used in place of a concentrated HCl solution. Inspection of the reactions after four days of resting revealed that crystals of the pure $\{Mo_{132}\}$ target had formed for reaction numbers 29 (cH) and 39 (dH). The small dark-brown polyhedral crystals were confirmed as $\{Mo_{132}\}$ by crystallographic unit-cell checks and by infrared and visible absorbance spectroscopy¹⁵.

Compounds **4** and **5** were isolated from the same reaction-screening array when the dithionite reducing agent was set at

10 mol% and the ratio of reduced molybdate: H_2SO_4 was varied across the scan. The original target for this screening-array scan was compound **5**, the $\{Mo_{368}\}$ 'lemon'¹⁶, as proof that even some of the most complex and hard-to-synthesize POM structures could be accessed using this screening methodology. However, in addition to finding conditions that crystallized this product successfully (reaction number 28, cI), conditions that crystallized **4**, a $\{Mo_{102}\}$ Keplerate ($Na_{12}[Mo(vi)_7Mo(v)_3O_{282}(SO_4)_{12}(H_2O)_{78}]$), were discovered (reaction number 29, cJ). This $\{Mo_{102}\}$ contains 12 sulfate ligands rather than the 12 acetate ligands as previously reported for the original $\{Mo_{102}\}$ structure^{24–26}. The isolation of $\{Mo_{102}\}$ and $\{Mo_{368}\}$ from the same array is an interesting observation as it provides new evidence that relates the structural aspects and synthetic conditions for these compounds. For details of the array conditions and product analyses see the Supplementary Information.

The potential to discover new POM clusters was demonstrated by isolating a polythioanion-based cluster with squaric acid as an organic template agent. Here we were inspired to explore the combination of $[Mo_2S_2O_2(H_2O)_6]^{2+}$, equal to an $\{Mo_2S_2O_2\}$ unit (first discovered and developed by Müller and co-workers²⁷ and then by Cadot and co-workers^{28–31}), with squaric acid to generate new POM architectures. As a result of the preliminary reaction scans using the screening array, we managed to isolate compound **6**, an unprecedented $\{Mo_{96}\}$ POM cluster that is triangular in shape and about 4 nm from apex to apex. The cluster has a 'triangle in a triangle' type of structure in which each of the triangles is capped by a

squarate group that bends to a $\{\text{Mo}_6\}$ -squarate group. Another six $\{\text{Mo}_6\}$ -squarate groups are ligated orthogonal to the plane of the triangle to complete this extraordinary structure type. The reaction-parameter space was explored in a similar fashion to those of the previous examples, with the $\{\text{Mo}_2\text{S}_2\text{O}_2\}$ stock solution varied with respect to the squaric acid template agent as well as the dilution factor.

After crystals of compounds 1–6 were obtained from each of their relative screening arrays, the reaction numbers provided a direct link, or ‘coordinates’, to the flow rates used to generate the solutions from which the target compounds crystallized. The pumps could therefore be programmed to run at these rates in a repetitive fashion to collect multiple batches of solutions with the desired compositions, and thus easily scale up the production of each of the target products. Over the multiple batches of crystallizations collected for compounds 1–3, the yields of crystalline material obtained remained consistently high throughout each set of batches. The average yield of $\{\text{Mo}_{36}\}$ from repeated batches of conditions 36 (dF) from the $\{\text{Mo}_{36}\}$ screening array was $78.7 \pm 5.3\%$ over ten reactions, the average yield of $\{\text{Mo}_{154}\}$ from repeated batches of conditions 25 (cE) from the $\{\text{Mo}_{154}\}$ screening array was $39.9 \pm 2.8\%$ over ten reactions and the average yield of $\{\text{Mo}_{132}\}$ from repeated batches of conditions 29 (cI) from the $\{\text{Mo}_{132}\}$ screening array was $49.4 \pm 4.4\%$ over ten reactions, all of which are consistent with those for the single-batch procedures previously reported in the literature^{13–16} (for individual batch yields, see Supplementary Figs S4–S6). The continuous production of uniform batch reactions in this manner therefore provided access to a reliable supply of large quantities of each of the target compounds.

To further demonstrate the general scope of this combined screening/scale-up approach we next targeted the synthesis and isolation of a range of coordination compounds of the form $\{\text{Mn}_3\}$ to $\{\text{Mn}_6\}$, compounds 7 to 10 (Fig. 5)^{17–20}. The magnetic properties of these compounds are of interest because oxime-based $\{\text{Mn}_x\}$ clusters are known to exhibit SMM behaviour^{8–12}. Indeed, the synthesis and physical analysis of SMMs is an area of intensive research within coordination chemistry because of the potential applications these materials may have in information storage, molecular spintronics, quantum computing and magnetic refrigeration^{32–37}. However, as with POMs, this increased attention has not led to the development of new synthetic methods beyond standard bench-top batch procedures, despite the SMM discovery, with synthetic scale-up being a major bottleneck that prevents the wider exploitation and investigation of such systems. The physical set-up of the pumps and tubing for the reactor system remained unchanged to that for the POM examples above, except that the POM reagent set was replaced by a set relevant to the various SMM syntheses (Fig. 5). The reagent set chosen for the SMM syntheses consisted of reagent-grade MeOH for dilution, 0.5 M $\text{Mn}(\text{ClO}_4)_2 \cdot 6\text{H}_2\text{O}$ in MeOH as the Mn source, 0.5 M triethylamine (TEA) in MeOH as the base and 0.25 M ethyl salicyloxime (Et-saoH₂) in MeOH, 1.5 M 4-*t*-butylpyridine (*t*BuPy) in MeOH and 0.125 M pivalic acid (piv) in MeOH as ligands. As with the POM-based systems, we were able to access the family of target clusters in a straightforward and rapid fashion (Fig. 5).

To scan the reaction parameters that surround the SMM compound 7, $\text{Mn}_3\text{O}(\text{Et-sao})_3(\text{MeOH})_3(\text{ClO}_4)$, the scanning programme applied was similar to that used for the POM syntheses. The starting point (reaction number 1, aA, Fig. 5) was set at an initial dilution ratio of 8:2 (that is, 80% MeOH and 20% reagent solutions by volume), the Mn:TEA ratio was set at a constant 1:1 by volume and the Et-saoH₂ ligand was set at 0%. The Et-saoH₂ content with respect to Mn and TEA by volume was then increased to 90% in increments of 10% across the first row of reactions. The second row (row b, Fig. 5) in the array began with the dilution ratio set to 6:4 and the Et-saoH₂ content reset to 0%. Then, the

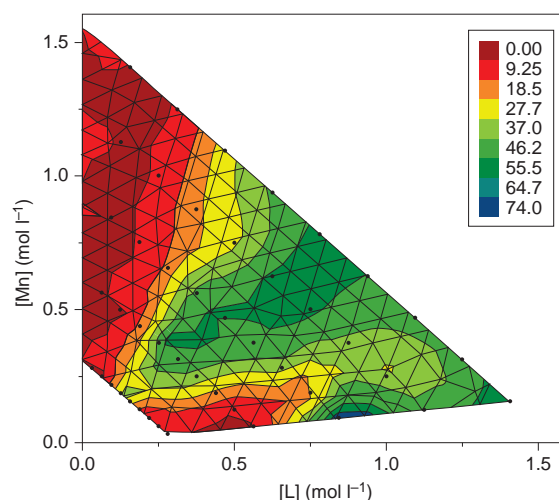


Figure 6 | Percentage yield as a function of manganese concentration $[\text{Mn}]$ and ligand concentration $[\text{L}]$ (mol l^{-1}) in the synthesis of compound 7. The trend shows that optimum yields are obtained when $[\text{Mn}]:[\text{L}] = 1:1$ and when both are greater than 0.25 mol l^{-1} .

ratio of Et-saoH₂ with respect to TEA and Mn was increased across each row of the array as the dilution factor decreased down the columns. Surprisingly, almost half of the 50 reactions in the array resulted in the formation of dark square/rectangular block crystals after resting for 4–5 days (characterized as compound 7 by crystallographic unit-cell checks and CHN elemental analysis). Owing to the large number of successful crystallizations from the array, a yield map for the product was calculated based on the theoretical Mn content for each reaction (Fig. 6 and Supplementary Fig. S7).

Inspection of the yield-map graphic shows a general trend of product yield increasing with concentration, but only when a ligand:Mn ratio of 1:1 is maintained. This is consistent with the product structure and with the conditions of the batch preparation reported originally¹⁷. However, the reported method in batch was reproduced and it was found that the optimum yield obtained under our screening conditions was about 20% higher than that given in the previously reported batch method¹⁷. The systematic exploration of the reaction landscape therefore allowed us to improve on the reported batch procedure by increasing the yield of the reaction. To extend this, similar reaction arrays were also set-up for compound 8 ($\text{Mn}_3\text{O}(\text{Et-sao})_3(\text{tBuPy})_3(\text{ClO}_4)$), compound 9 ($\text{Mn}_5\text{O}_2(\text{Et-sao})_6(\text{MeO})(\text{H}_2\text{O})(\text{MeOH})_2$) and compound 10 ($\text{Mn}_6\text{O}_2(\text{Et-sao})_6(\text{piv})_2(\text{MeOH})_6$). For compound 8, the starting point (reaction number 1, aA) was set at an initial dilution ratio of 8:2 (that is, 80% MeOH and 20% reagent solutions by volume), the Et-saoH₂:Mn:TEA ratio was set at a constant 2:1:1 by volume and the *t*BuPy ratio was set at 0%. Variation of the *t*BuPy and the dilution ratio subsequently led to the successful crystallization of compound 8 for a number of reactions in the array output. Compounds 9 and 10 were obtained similarly by variation of the other ligand sources with respect to the Et-saoH₂, Mn and TEA reagents (see Supplementary Figs S8–S10 for yield maps of compounds 8, 9 and 10).

Conclusions

In this report a new approach to screen and scale up the synthetic conditions for a number of inorganic clusters using an automated adjustment of flow rates of precursor reagent solutions is established. The syntheses of a selection of polyoxomolybdate structures were first scanned using the flow-system array as an initial proof of concept for the automated screening process.

Then, the successful reaction conditions obtained from the screening process were applied continuously to demonstrate the ability to increase easily the quantity of material produced. Application of the synthetic approach to obtain a small family of oxime-based Mn SMMs further demonstrated the scope for the possible expansion and use of this technology across the entire field of coordination chemistry. The ability to use such methods in cluster synthesis demonstrates the potential of this approach to change the way in which inorganic cluster materials are discovered and their syntheses optimized. Furthermore, the adoption of this technology by researchers in these areas could ideally enable them to take full advantage of the advances in online solution-based analytical techniques currently being developed for flow-based methodologies^{38–43}. Eventually, this could lead to a fully automated reaction set-up capable of the discovery, optimization and scale up of syntheses for new inorganic clusters, and possibly even extend it to other types of systems that traditionally use one-pot self-assembly reactions. Our future work aims to build on the isolation of the novel {Mo₉₆} POM cluster and explore the application of the flow-system array to the discovery of other new inorganic clusters.

Methods

All chemicals were of analytical reagent grade purchased from Sigma Aldrich, Fisher Scientific and Alfa Aesar chemical companies and used as supplied, without further purification. The standard stock solutions of each reagent were prepared using standard practices and volumetric glassware. All solutions were prepared with deionized water and stored in plastic labware after preparation, except for the reducing-agent stocks, which were freshly prepared (less than one hour) prior to each experiment run and {Mo₂} stock solution, which was prepared according to previous reports³¹.

Pump system. The pump-system set up utilized between three and 12 programmable syringe pumps (C3000 model, Tricontinent) fitted with a 5 ml syringe and a three-way solenoid valve; a LabVIEWTM-based PC interface was used to control the pumps. FEP plastic tubing of 1/8 inch (3.175 mm) outer diameter was cut to the specified lengths and connected using standard HPLC low-pressure polytetrafluoroethylene connectors and a PEEK manifold (Thames Restek).

General procedure for the generation of reaction arrays. All reaction arrays were carried out using the following general procedures. Stock solutions of reagents were prepared and connected to the inlets for the assigned pumps. The connective tubing and pumps for all reagents were purged with the reagent solutions (3 ml) and the reactor tubing then flushed clean with fresh solvent (20 ml). Next, the prewritten command scripts were executed to initiate the pumping sequence (see the Supplementary Information). The 50 individual reaction batches were collected, and the test tubes changed manually at each programmed refill point. To take account of the reactor tubing volume, the first two reaction volumes collected were always discarded and two extra volumes of solvent were used to purge the reactor line at the end of each sequence. The samples collected were then left undisturbed for the specified resting period to allow crystallization of the products. Full structural data for compounds **4**, **6** and **9** are given in the Supplementary Information.

Received 6 February 2012; accepted 28 September 2012;
published online 18 November 2012

References

- Luis, S. V. & Garcia-Verdugo, E. *Chemical Reactions and Processes under Flow Conditions* (Royal Society of Chemistry, 2010).
- Seeberger, P. H. Organic synthesis: scavengers in full flow. *Nature Chem.* **1**, 258–260 (2009).
- Wegner, J., Ceylan, S. & Kirschning, A. Ten key issues in modern flow chemistry. *Chem. Commun.* **47**, 4583–4592 (2011).
- Hartman, R. L., McMullen, J. P. & Jensen, K. F. Deciding whether to go with the flow: evaluating the merits of flow reactors for synthesis. *Angew. Chem. Int. Ed.* **50**, 7502–7519 (2011).
- Abou-Hassan, A., Sandre, O. & Cabuil, V. Microfluidics in inorganic chemistry. *Angew. Chem. Int. Ed.* **49**, 6268–6286 (2010).
- Long, D.-L., Burkholder, E. & Cronin, L. Polyoxometalate clusters, nanostructures and materials: from self assembly to designer materials and devices. *Chem. Soc. Rev.* **36**, 105–121 (2007).
- Long, D.-L., Tsunashima, R. & Cronin, L. Polyoxometalates: building blocks for functional nanoscale systems. *Angew. Chem. Int. Ed.* **49**, 1736–1758 (2010).
- Evangelisti, M. & Brechin, E. K. Recipes for enhanced molecular cooling. *Dalton Trans.* **39**, 4672–4676 (2010).
- Inglis, R., Milios, C. J., Jones, L. F., Piligkos, S. & Brechin, E. K. Twisted molecular magnets. *Chem. Commun.* **48**, 181–190 (2012).
- Moushi, E. E. *et al.* Inducing single-molecule magnetism in a family of loop-of-loops aggregates: heterometallic Mn₄₀Na₄ clusters and the homometallic Mn₄₄ analogue. *J. Am. Chem. Soc.* **132**, 16146–16155 (2010).
- Murrie, M. Cobalt(II) single-molecule magnets. *Chem. Soc. Rev.* **39**, 1986–1995 (2010).
- Wang, X.-Y., Avendano, C. & Dunbar, K. R. Molecular magnetic materials based on 4d and 5d transition metals. *Chem. Soc. Rev.* **40**, 3213–3238 (2011).
- Krebs, B., Stiller, S., Tytko, K. H. & Mehmke, J. Structure and bonding in the high-molecular-weight isopolymolybdate ion, (Mo₃₆O₁₁₂(H₂O)₁₆)⁸⁻ – the crystal structure of Na₈(Mo₃₆O₁₁₂(H₂O)₁₆)·58H₂O. *Eur. J. Solid State Inorg. Chem.* **28**, 883–903 (1991).
- Müller, A. *et al.* Rapid and simple isolation of the crystalline molybdenum-blue compounds with discrete and linked nanosized ring-shaped anions: Na₁₅[Mo₁₂₆Mo₂₈O₄₆₂H₁₄(H₂O)_{701.5}][Mo₁₂₄Mo₂₈O₄₅₇H₁₄(H₂O)_{681.0.5}]·ca.400H₂O and Na₂₂[Mo₁₁₈Mo₂₈O₄₄₂H₁₄(H₂O)₅₈]·ca.250H₂O. *Z. Anorg. Allg. Chem.* **625**, 1187–1192 (1999).
- Müller, A., Krickemeyer, E., Bögge, H., Schmidtman, M. & Peters, F. Organizational forms of matter: an inorganic super fullerene and Keplerate based on molybdenum oxide. *Angew. Chem. Int. Ed.* **37**, 3359–3363 (1998).
- Müller, A., Beckmann, E., Bögge, H., Schmidtman, M. & Dress, A. Inorganic chemistry goes protein size: a Mo₃₆₈ nano-hedgehog initiating nanochemistry by symmetry breaking. *Angew. Chem. Int. Ed.* **41**, 1162–1167 (2002).
- Inglis, R. *et al.* Enhancing SMM properties via axial distortion of Mn₃^{III} clusters. *Chem. Commun.* **45**, 5924–5926 (2008).
- Inglis, R. *et al.* Twisting, bending, stretching: strategies for making ferromagnetic [Mn₃^{III}] triangles. *Dalton Trans.* **42**, 9157–9168 (2009).
- Inglis, R. *et al.* Attempting to understand (and control) the relationship between structure and magnetism in an extended family of Mn₆ single-molecule magnets. *Dalton Trans.* **18**, 3403–3412 (2009).
- Kozoni, C., Siczek, M., Lis, T., Brechin, E. K. & Milios, C. J. The first amino acid manganese cluster: a [Mn₂^{IV}Mn₃^{III}] DL-valine cage. *Dalton Trans.* **42**, 9117–9119 (2009).
- Levenspiel, O. *Chemical Reaction Engineering* (John Wiley, 1999).
- Müller, A. *et al.* [Mo₁₅₄(NO)₁₄O₄₂₀(OH)₂₈(H₂O)₇₀]^{(25±5)-}: a water-soluble big wheel with more than 700 atoms and a relative molecular mass of about 24000. *Angew. Chem. Int. Ed. Engl.* **34**, 2122–2124 (1995).
- Müller, A., Meyer, J., Krickemeyer, E. & Diemann, E. Molybdenum blue: a 200 year old mystery unveiled. *Angew. Chem. Int. Ed. Engl.* **35**, 1206–1208 (1996).
- Müller, A. *et al.* Thirty electrons ‘trapped’ in a spherical matrix: a molybdenum oxide-based nanostructured Keplerate reduced by 36 electrons. *Angew. Chem. Int. Ed.* **39**, 1614–1616 (2000).
- Müller, A. *et al.* Drawing small cations into highly charged porous nanocounters reveals ‘water’ assembly and related interaction problems. *Angew. Chem. Int. Ed.* **42**, 2085–2090 (2003).
- Henry, M., Bögge, H., Diemann, E. & Müller, A. Chameleon water: assemblies confined in nanocapsules. *J. Mol. Liq.* **118**, 155–162 (2005).
- Rittner, W., Müller, A., Neumann, A., Bafher, W. & Sharma, R. C. Generation of the triangulo-group Mo^V-ETA-S₂ in the condensation of [Mo^{VI}O₂S₂]₂ to [Mo^VO₂S₂]₂. *Angew. Chem. Int. Ed. Engl.* **17**, 530–531 (1979).
- Cadot, E., Salignac, B., Halut, S. & Sécheresse, F. [Mo₁₂S₁₂O₁₂(OH)₁₂(H₂O)₆]: a cyclic molecular cluster based on the [Mo₂S₂O₂]²⁺ building block. *Angew. Chem. Int. Ed.* **37**, 611–612 (1998).
- Salignac, B., Riedel, S., Dolbecq, A., Sécheresse, F. & Cadot, E. ‘Wheeling templates’ in molecular oxothiomolybdate rings: syntheses, structures, and dynamics. *J. Am. Chem. Soc.* **122**, 10381–10389 (2000).
- Cadot, E., Salignac, B., Marrot, J., Dolbecq, A. & Sécheresse, F. [Mo₁₀S₁₀O₁₀(OH)₁₀(H₂O)₅]: a novel decameric molecular ring showing supramolecular properties. *Chem. Commun.* 261–262 (2000).
- Cadot, E., Salignac, B., Halut, S. & Sécheresse, F. [Mo₁₂S₁₂O₁₂(OH)₁₂(H₂O)₆]: a cyclic molecular cluster based on the [Mo₂S₂O₂]²⁺ building block. *Angew. Chem. Int. Ed.* **37**, 611–613 (1998).
- Bogani, L. & Wernsdorfer, W. Molecular spintronics using single-molecule magnets. *Nature Mater.* **7**, 179–186 (2008).
- Evangelisti, M., Luis, F., de Jongh, L. J. & Affronte, M. Magnetothermal properties of molecule-based materials. *J. Mater. Chem.* **16**, 2534–2549 (2006).
- Zheng, Y.-Z., Evangelisti, M., Tuna, F. & Wippeny, R. E. P. Co–Ln mixed-metal phosphonate grids and cages as molecular magnetic refrigerants. *J. Am. Chem. Soc.* **134**, 1057–1065 (2012).
- Leuenberger, M. N. & Loss, D. Quantum computing in molecular magnets. *Nature* **410**, 789–793 (2001).
- Lehmann, J., Gaita-Arino, A., Coronado, E. & Loss, D. Spin qubits with electrically gated polyoxometalate molecules. *Nature Nanotechnol.* **2**, 312–317 (2007).

37. Karotsis, G. *et al.* [Mn^{III}₄Ln^{III}₄] calix[4]arene clusters as enhanced magnetic coolers and molecular magnets. *J. Am. Chem. Soc.* **132**, 12983–12990 (2010).
38. Lange, H. *et al.* A breakthrough method for the accurate addition of reagents in multi-step segmented flow processing. *Chem. Sci.* **2**, 765–769 (2011).
39. McMullen, J. P., Stone, M. T., Buchwald, S. L. & Jensen, K. F. An integrated microreactor system for self-optimization of a heck reaction: from micro- to mesoscale flow systems. *Angew. Chem. Int. Ed.* **49**, 7076–7080 (2010).
40. Parrott, A. J., Bourne, R. A., Akien, G. R., Irvine, D. J. & Poliakoff, M. Self-optimizing continuous reactions in supercritical carbon dioxide. *Angew. Chem. Int. Ed.* **50**, 3788–3792 (2011).
41. Rasheed, M. & Wirth, T. Intelligent microflow: development of self-optimizing reaction systems. *Angew. Chem. Int. Ed.* **50**, 357–358 (2011).
42. Miras, H. N. *et al.* Unveiling the transient template in the self assembly of a molecular oxide nano-wheel. *Science* **327**, 72–74 (2010).
43. Miras, H. N., Richmond, C. J., Long, D.-L. & Cronin, L. Solution-phase monitoring of the structural evolution of a molybdenum blue nanoring. *J. Am. Chem. Soc.* **134**, 3816–3824 (2012).

Acknowledgements

This work was supported by the Engineering and Physical Sciences Research Council, WestCHEM, The Leverhulme Trust and the University of Glasgow. L.C. thanks the Royal Society/Wolfson Foundation for a merit award. H.N.M. thanks the Royal Society of

Edinburgh and Marie Curie Actions for financial support. We also thank J. McIver for technical assistance in assembling the electronics and flow kit.

Author contributions

L.C. conceived the overall idea and designed the flow system, including the control concept. L.C. and C.J.R. designed experiments, analysed data, prepared the figures and co-wrote the manuscript. H.N.M. helped with some of the flow-system design, provided advice and assisted with crystallography. A.R. applied and corroborated the syntheses and compound analysis. D.L. solved and checked the crystallographic data. C.J.R. and L.P. co-wrote the software interface used for the programmed pump control and C.M. helped in the verification of the interface. E.K.B and R.I. provided help with the synthesis of the Mn-based complexes. V.S. provided help with chemical engineering aspects and H.Z. helped with the synthesis of compound **6**.

Additional information

Supplementary information is available in the online version of the paper. Reprints and permission information is available online at <http://www.nature.com/reprints>. Correspondence and requests for materials should be addressed to L.C.

Competing financial interests

The authors declare no competing financial interests.